Imaging Neuroscience
an open access journal

Research Article

Systematic cross-sectional age-associations in global fMRI signal topography

Jason S. Nomi[a,*], Danilo Bzdok[b,*], Jingwei Li[c,d], Taylor Bolt[a], Catie Chang[e], Salome Kornfeld[f], Zachary T. Goodman[g], B.T. Thomas Yeo[h], R. Nathan Spreng[i,j], Lucina Q. Uddin[a,k]

[a]Department of Psychiatry and Biobehavioral Sciences, University of California, Los Angeles, CA, United States
[b]Department of Biomedical Engineering, Montreal Neurological Institute (MNI), Brain-imaging institute (BIC), McGill University, Montreal, QC, Canada; Mila - Quebec Artificial Intelligence Institute, Quebec, Canada
[c]Institute of Neuroscience and Medicine (INM-7: Brain and Behavior), Research Center Jülich, Jülich, Germany
[d]Institute of Systems Neuroscience, Medical Faculty and University Hospital Düsseldorf, Heinrich Heine University Düsseldorf, Düsseldorf, Germany
[e]Departments of Electrical and Computer Engineering, Computer Science, and Biomedical Engineering, Vanderbilt University, Nashville, TN, United States
[f]Reha Rheinfelden, Rheinfelden, Switzerland
[g]Department of Psychology, University of Miami, Coral Gables, FL, United States
[h]Centre for Sleep & Cognition, Centre for Translational MR Research, Electrical and Computer Engineering, N.1 Institute for Health & Institute for Digital Medicine, National University of Singapore, Singapore
[i]Laboratory of Brain and Cognition, Montreal Neurological Institute, Department of Neurology and Neurosurgery, McGill University, Montreal, QC, Canada
[j]Departments of Psychiatry and Psychology, McGill University, Montreal, QC, Canada
[k]Department of Psychology, University of California, Los Angeles, CA, United States

*These authors contributed equally

Corresponding Author: Jason S. Nomi (jnomi@mednet.ucla.edu)

ABSTRACT

The global signal (GS) in resting-state functional MRI (fMRI), known to contain artifacts and non-neuronal physiological signals, also contains important neural information related to individual state and trait characteristics. Here, we show distinct linear and curvilinear relationships between GS topography and age in a cross-sectional sample of individuals (6-85 years old) representing a significant portion of the lifespan. Subcortical brain regions such as the thalamus and putamen show linear associations with the GS across age. The thalamus has stronger contributions to the GS in older-age individuals compared with younger-aged individuals, while the putamen has stronger contributions in younger individuals compared with older individuals. The subcortical nucleus basalis of Meynert shows a u-shaped pattern similar to cortical regions within the lateral frontoparietal network and dorsal attention network, where contributions of the GS are stronger at early and old age, and weaker in middle age. This differentiation between subcortical and cortical brain activity across age supports a dual-layer model of GS composition, where subcortical aspects of the GS are differentiated from cortical aspects of the GS. We find that these subcortical-cortical contributions to the GS depend strongly on age across the lifespan of human development. Our findings demonstrate how neurobiological information within the GS differs across development and highlight the need to carefully consider whether or not to remove this signal when investigating age-related functional differences in the brain.

Keywords: aging, artifact removal, brain development, denoising strategies, intrinsic functional connectivity, frontoparietal network, signal versus noise

Received: 26 August 2023 Revision: 29 January 2024 Accepted: 31 January 2024 Available Online: 16 February 2024

1. INTRODUCTION

One of the biggest challenges in neuroscience is separating signal from noise (Uddin, 2020). In functional neuroimaging generally, and in human connectomics investigations using resting-state functional MRI (fMRI) data specifically, this challenge has been addressed with processing pipelines that mitigate artifacts known to obscure neural signals (Ciric et al., 2017; Parkes et al., 2018). The goal of these processing steps is to differentiate noise and relevant neural signals in fMRI data by removing physiological, hardware, and head motion-related signals to permit the discovery of underlying functional network architectures in the human brain. The "global signal" (GS) refers to the time series of signal intensity averaged across all voxels covering the brain, yielding one aggregate statistic per subject. The process of GS regression has been widely adopted as a robust method for attenuating noise due to cardiac and respiratory events and other confounding signals (Power et al., 2017). GS regression can also improve functional connectivity (FC) prediction of behavior (Li, Kong, et al., 2019). However, the GS is also an important component of brain function. Simultaneous fMRI-intracranial EEG studies in macaque monkeys demonstrate that gamma-band cortical electrical activity exhibits a positive correlation with BOLD changes across the entire cerebral cortex (Schölvinck et al., 2010) and unilateral suppression of the cholinergic basal forebrain causes changes in GS topography (Turchi et al., 2018). Simultaneous measurement of resting-state fMRI and calcium activity in awake rats has demonstrated significant correspondence between the GS measured non-invasively and neural spiking activity (Ma et al., 2020). Taken together, the emerging picture from these studies suggests that the GS contains relevant neural components, and does not simply represent noise in neuroscience investigations (Bolt et al., 2022; Li, Bolt, et al., 2019).

The GS has also been shown to contain important information related to behavioral traits and intrinsic network organization in humans. We previously demonstrated that GS topography was related to a population axis of positive and negative life outcomes and psychological function, particularly weighted in frontoparietal executive control network regions, in a sample of over 1000 22-37 year old adults (Li, Bolt, et al., 2019). Positive and negative life outcomes included measures of education, life satisfaction, cognitive flexibility, aggressive and internalizing behavior, alcohol abuse, and antisocial personality among others. More recently, we have shown that a dynamic spatiotemporal pattern that explains ~20% of resting-state BOLD variance has a time series signature that is almost perfectly correlated (r = 0.97) with the GS (Bolt et al., 2022). This spatiotemporal pattern consists of negative cortex-wide BOLD amplitudes within the somato-motor-visual (SMLV) complex, that then propagate toward cortical regions overlapping primarily with the frontoparietal network (FPN), but also with the default network (DN) and primary visual cortex (V1), followed by a spatiotemporal sequence with positive BOLD amplitudes with the same dynamics. These findings further suggest that the resting-state fMRI GS contains a rich source of important information relevant to large-scale brain network functional organization and individual differences in human cognition and behavior.

These results fit with the more recent conception of the GS as an important source of neural information, rather than being solely a source of noise. Accordingly, a recently developed dual-layer model of GS composition proposes that the GS represents two different layers of brain function (Zhang & Northoff, 2022). The first is a background subcortical-cortical layer where cortical activity is modulated by arousal and vigilance via subcortical regions such as the thalamus, basal forebrain, and midbrain. The second is a foreground cortico-cortical layer that is represented by network integration and segregation that is associated with cognitive states during rest and task. These two layers may operate in concert or independently to facilitate brain activity. This dual-layer model of the GS helps to reconcile the involvement of the GS in arousal, physiology, and cognition. However, it is currently unclear how subcortical and cortical brain activity contributing to the GS may differ across early and later life stages.

Here, we undertake a comprehensive assessment of age-related changes in spatial topography of brain regions associated with the GS from 6-85 years of age. Despite the large amount of attention given to characterizing GS topography (for a review see: Ao et al., 2021) and the impact of GS regression on some of the most commonly deployed preprocessing pipelines (Ciric et al., 2017; Parkes et al., 2018; Power et al., 2017), the question of how age shapes the topography of the GS has not been carefully considered. Consequently, the extent that existing findings documenting changes in large-scale functional brain network configuration across age are potentially confounded with the differential implementation of GS regression across research groups is entirely unknown. We find distinct GS topography associations with age that were reliably present across multiple fMRI data preprocessing procedures. The findings suggest that the GS conveys neurobiologically meaningful information that changes over the course of human development, and that developmental and aging studies choosing to implement GS regression warrant careful reconsideration.

2. MATERIALS AND METHODS

2.1. Subjects and fMRI data

A 10-minute resting-state fMRI scan was obtained from 601 subjects (6-85 years old; 240 males; Supplementary Fig. 1) without a current Diagnostic and Statistical Manual of Mental Disorders (DSM) diagnosis from the Nathan Kline Institute (NKI) enhanced publicly available data repository (Nooner et al., 2012) (http://fcon_1000.projects.nitrc.org/indi/enhanced/). All participants provided written informed consent (written assent was obtained from minors and their legal guardian) for their data to be shared anonymously through the International Neuroimaging Data-Sharing Initiative (INDI) website (http://fcon_1000.projects.nitrc.org/). Brain imaging was performed on a Siemens Trio 3.0 T scanner that collected a T1 anatomical image and multiband (factor of 4) EPI sequenced resting-state fMRI data (2x2x2 mm, 40 interleaved slices, TR = 1.4 s, TE = 30 ms, flip angle = 65°, FOV = 224 mm, 404 volumes; ~9 minutes and 19 seconds). Participants were instructed to keep their eyes open and fixate on a cross centered on the screen. For quality control, we ensured that all participants had less than 0.5 mm average framewise displacement (FD). Linear regression revealed a significant linear FD-age association ($\beta = 0.35$, $p = 1.23E\text{-}18$) but no significant quadratic FD-age association ($p = 0.9$). Therefore, head motion was used as a nuisance covariate in all analyses.

2.2. Preprocessing pipelines

To account for non-neuronal artifacts and head motion, analyses were conducted across several preprocessing pipelines (MP - minimally preprocessed; CR - covariate regression; ICA-FIX; temporal ICA (tICA)). Spatial ICA denoising, on which ICA-FIX is based, has been identified as one of the most effective tools for removing spatially structured noise artifacts from fMRI data (Ciric et al., 2018; Parkes et al., 2018). We also applied temporal ICA (tICA), which complements spatial ICA by removing temporally structured global noise (Glasser et al., 2018). Collectively, these methods were investigated to ensure that non-neuronal artifacts were not driving the age associations with GS topography. These preprocessing pipelines were implemented to demonstrate that GS topography associations with age are robust to a range of widely-used denoising procedures.

2.3. Minimally preprocessed (MP) pipeline

All resting-state fMRI data were preprocessed using FSL, AFNI, and SPM functions through DPARSF-A in DPABI (Yan & Zang, 2010). The first five images were removed to allow the MRI signal to reach equilibrium. Next, resting-state fMRI data were despiked using AFNI 3dDespike, realigned, and normalized with DPARSF-A into 3 mm MNI space using a priori SPM EPI templates, smoothed using AFNI 3dBlurToFWHM (6 mm), and bandpass filtered using DPARSF-A (0.01 - 0.1 Hz).

2.4. Covariate regression (CR) pipeline

After smoothing, DPARSF-A was used to calculate and regress out nuisance variables for covariate regression (CR) consisting of 24 motion parameters (six rigid-body head motion parameters, the previous time point for all six parameters, and the 12 squared derivatives; Friston et al., 1996), white matter time-series and cerebral spinal fluid time-series (using DPABI default masks), and a linear detrend. Finally, the data were bandpass filtered (0.01 - 0.1 Hz).

2.5. ICA-FIX denoising

Subject-level spatial ICA denoising (Griffanti et al., 2014) was conducted using ICA-FIX on minimally preprocessed data that were smoothed, but not subjected to covariate regression or bandpass filtering. The ICA-FIX classifier was trained on hand-classified independent components separated into noise and non-noise categories on data from 24 subjects (randomly sampled by choosing subjects separated by ~10 years of age, with small and large amounts of head motion). Noise and non-noise components were classified by visual inspection using component maps, time-series, and power spectra (Griffanti et al., 2017). The resulting component classifications were then fed into FMRIB's ICA-FIX classification algorithm (Salimi-Khorshidi et al., 2014) to automatically classify noise and non-noise components from individual subject data. Next, components classified as noise were regressed out of the data. Finally, the 24 motion parameters and a linear trend were regressed out of the data, before a bandpass filter (0.01 - 0.1 Hz) was applied.

2.6. Temporal independent component analysis (tICA) denoising

The temporal ICA (tICA) pipeline was conducted using the FastICA algorithm in Python (https://scikit-learn.org/stable/modules/generated/sklearn.decomposition.FastICA.html). The tICA pipeline first conducted a group spatial ICA (sICA) on all 601 resting-state scans, producing 125 independent components (Glasser et al., 2018; Smith et al., 2012; Supplementary Figs. 2-6). Classification of noise and non-noise components was conducted according to the procedure detailed in the ICA-FIX

pipeline. Thirty-nine sICA components classified as noise were then regressed out of the remaining 86 non-noise sICA component time-courses. The cleaned time-courses from the sICA were then concatenated across subjects to produce 86 time-courses, each with 239,799 TRs (399 TRs x 601 subjects). These concatenated cleaned sICA time-courses and representative group component spatial maps were then subjected to a tICA that produced 75 tICA time-courses and the associated group tICA spatial component maps (Supplementary Figs. 7 and 8).

Temporal ICA components can be classified just as spatial ICA components with visual identification of network activity and noise (Glasser et al., 2018). Nineteen of the 75 tICA components were identified as noise (Supplementary Fig. 9). These components consisted of anti-correlated activity within the brain stem (e.g., TC 2, TC 17, TC 18) and striped banding representing head motion (e.g., TC 14, TC 28). Temporal ICA component 72 (Supplementary Fig. 9) showed a general overall negativity across the cortex with little anti-correlation. Such tICA components in previous work have been proposed to represent a global component thought to be associated with the noise aspects of the GS (Glasser et al., 2018; Smith et al., 2012). Finally, the time-series from the 19 group tICA noise components, the 39 group sICA noise components, the Friston 24 motion parameters, and a linear detrend were regressed out of each subject's resting-state data before a bandpass filter was applied.

2.7. Scrubbing

Frames where FD exceeded 0.5 mm (Power et al., 2012) were not included in the regression model (average number of scrubbed frames per subject was 31.43 of 399 TRs (12.70%; range 0 - 204 TRs; 204 TRs = 285.6 seconds or ~4 minutes and 45 seconds)). There was a significant linear (β = 0.27, p = 4.289e-12) association between total number of scrubbed frames and age but no quadratic association (p = 0.69). All preprocessing pipelines were examined with and without scrubbing.

2.8. Global signal topography and the general linear model

The GS was calculated as the mean time-series of all gray matter voxels within an SPM gray matter probability mask thresholded at 20%. Previous research has shown that the GS calculated across all voxels (white matter, CSF, etc.) in the brain compared to the GS calculated across only gray matter voxels in the brain are nearly identical (Glasser et al., 2018; Li, Bolt, et al., 2019), making it unlikely that the current methodology influenced the results. Linear regression between the GS time-series and the time-series of each voxel produced whole-brain voxel-wise beta maps. Frames where FD (Power et al., 2012) exceeded 0.5 mm were not included in the regression model for preprocessing pipelines with scrubbing. Next, each individual subject's beta map was converted to z-statistics. Two general linear models (GLM) were then run in FSL using the whole-brain voxel-wise beta maps for all participants as the dependent variable (DV). The first GLM included linear age, mean FD, and sex as independent variables (IV) while the second GLM included linear age, quadratic age, mean FD, and sex as IVs. Age was the IV of interest within the first model, and quadratic age was the IV of interest within the second model. The resulting group spatial maps were thresholded in FSL (voxel-wise uncorrected at $p < 0.001$ and cluster-wise corrected at $p < 0.05$) using Gaussian Random Field (GRF) theory. The two GLMs were run across all preprocessing pipelines.

3. RESULTS

3.1. Global signal topography across early and later life stages

The main results presented in Figures 1-3 are from the tICA pipeline. Global signal topography maps showed increased contributions of visual, frontal, and sensorimotor brain regions to the GS across age (Fig. 1). GLM results show that GS topography has distinct cross-sectional associations across early and later life stages across subcortical and cortical brain regions. For subcortical brain regions, the thalamus shows a strong positive linear relationship with age, where associations between the thalamus and GS time-series (scatterplot represents voxels within the thalamus thresholded at $z > 5$ for presentation purposes) increased across age (Fig. 2). The nucleus basalis (-18, -2, -12) was identified using the localization from a previous GS study (X. Liu et al., 2018) and showed a positive quadratic effect, where association with the GS was weakest during middle age but stronger in young and old age. Finally, the putamen showed a negative linear relationship with age where association with the GS is strongest in early age but weakest during old age. These results demonstrate that subcortical regions involved in arousal and vigilance have distinct age-dependent cross-sectional associations with the GS across early and later life stages.

For cortical brain regions, the lateral frontoparietal control network (parietal cortex overlapping with Schaefer ROI 333) (17 Network 400 ROI parcellation; Schaefer et al., 2018), dorsal attention network (inferior temporal cortex overlapping with Schaefer ROI 271, 272; FEF overlapping

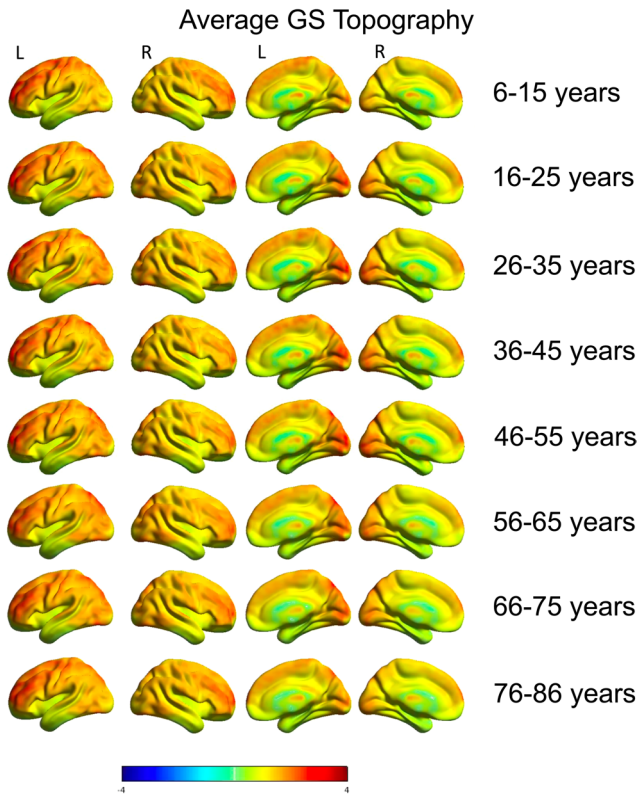

Fig. 1. Average global signal topography across 10-year age groups. Increased associations between the GS with visual, sensorimotor, and prefrontal cortical regions are found across each age group.

with Schaefer ROI 61, 261) showed a quadratic association with the GS where network nodes coupled with the GS are strongest at early (<20 years) and later (>60 years) periods of life, and the weakest in middle age (Fig. 3). These results demonstrate distinct age-dependent large-scale network associations with the GS in networks related to external attention and cognition such as the control network and dorsal attention network.

3.2. Preprocessing pipelines and imaging artifacts

Both linear and quadratic associations between GS topography and age were largely unaffected by preprocessing choices and produced the same linear and quadratic cross-sectional age effects as the main analysis (Supplementary Figs. 10 and 11). More conservative and liberal classifications of tICA noise components (that did and did not include tICA component 72 (Supplementary Fig. 9) produced similar results to the original 19 noise-component classification presented here. Additionally, non-scrubbed analyses that were also run for all four preprocessing pipelines showed no differences in linear and quadratic associations when compared with the main analyses that employed volume scrubbing (Supplementary Fig. 12). This shows that the noise and non-noise classification criteria of tICA components and the inclusion or exclusion of volume scrubbing did not influence the pattern of results presented here.

In order to ensure that different preprocessing pipelines did change the composition of the GS time-series while leaving GS topography cross-sectional effects with age generally unaffected, within-subject temporal correlations between GS time-series across different preprocessing pipelines were calculated. The within-subject average GS time-series showed a strong temporal correlation across all preprocessing pipelines (rs = 0.73 - 0.96) (Fig. 4). The temporal correlation of the GS time-series between the FIX pipeline and the tICA pipeline was r = 0.76. The lower correlation between the FIX and tICA pipelines shows that the addition of tICA denoising has a large influence on the composition of the GS, demonstrating that a large amount of variance was removed (r = 0.76; R^2 = 58% variance explained). This demonstrated the effectiveness of tICA denoising in removing spatially and temporally structured fMRI noise within resting-state data that contribute to the GS, and also demonstrates the robustness of the current GS topography-age effects.

Despite the large amount of variance removed from tICA denoising compared with ICA-FIX in the GS time-series, the within-subject GS topography spatial map correlations showed little changes between the FIX pipeline and the tICA denoising pipeline (r = 0.96). This demonstrates that spatially and temporally structured noise do not significantly contribute to GS topography composition (Fig. 4); if spatially and temporally structured noise did have an influence on GS topography, the within-subject spatial map correlation between the FIX and tICA pipelines should be much lower. Thus, although tICA denoising results in a quantifiable change in the GS time-series composition, GS topography remains unaffected.

Group-level spatial correlations between the voxel-wise GLM linear and quadratic spatial map outputs were used to quantify the influence of preprocessing pipeline on age effects. These results showed that spatial patterns of linear (rs = 0.81 - 0.97) and quadratic (rs = 0.77 - 0.97) GS topography GLM results for age effects are similar across preprocessing pipelines (Fig. 4). Thus, while the tICA preprocessing pipeline removes a significant amount of GS time-series variability, the within-subject GS spatial topography and group GLM GS spatial topography cross-sectional age effects remain relatively stable.

3.3. Head motion and other considerations

Scatterplots showing the relationship between FC strength and head motion (i.e., FD) plotted according to

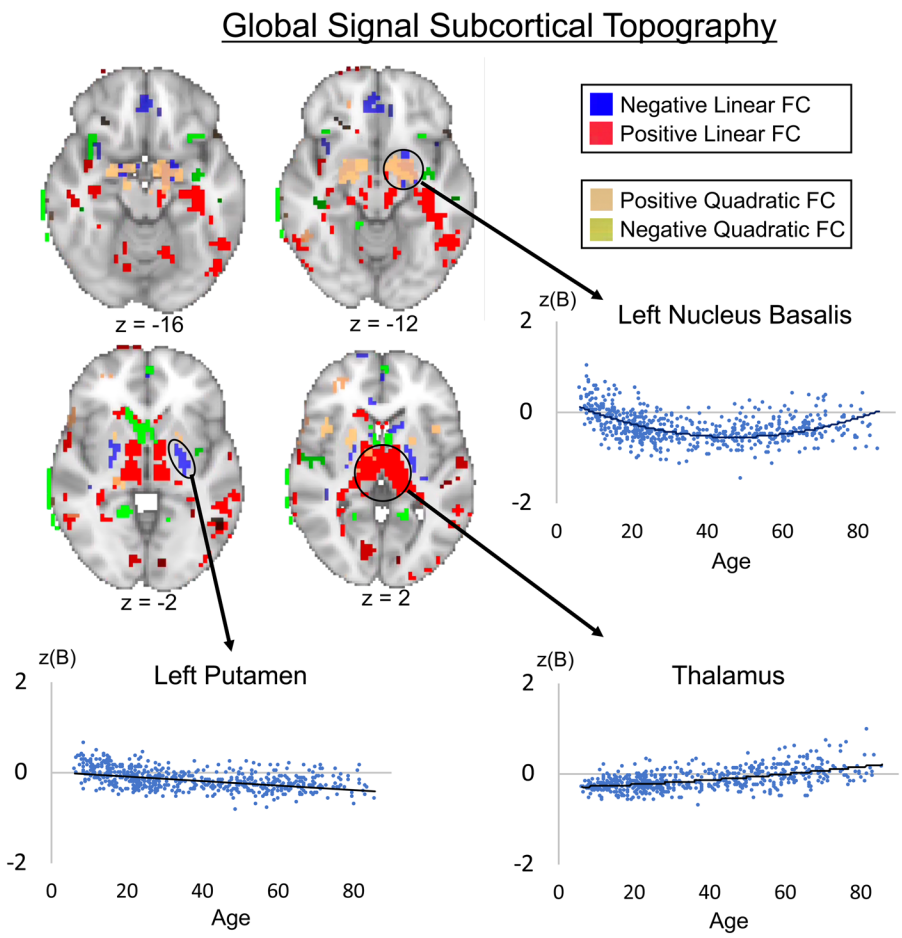

Fig. 2. Group spatial maps showing subcortical associations between the global signal and voxel-wise time-series across age ($p < 0.001$ voxel-wise uncorrected and $p < 0.05$ cluster-wise corrected). Negative quadratic associations show that the global signal has weaker associations with the nucleus basalis in middle-aged individuals compared with younger and older individuals. The thalamus shows a positive linear association, where association with the GS is stronger in older individuals compared with younger individuals. The putamen shows a negative linear association where association with the GS is stronger in younger individuals compared with older individuals. The z-scored unstandardized beta is on the y-axis and age is on the x-axis.

spatial distance between ROIs were used to determine if head motion was producing the distance-dependence effect where short-range FC strength shows a negative association with FD and long-range FC strength shows a positive association with FD. The time-series from each ROI within the 400 ROI 17 network Schaefer parcellation (Schaefer et al., 2018) were correlated across network node pairs to create a correlation matrix for each subject. Each connection was correlated with FD values across all subjects and then placed on the scatterplot according to the euclidean distance between each ROI. The scatterplots show that there is no distance-dependence effect of head motion for any preprocessing pipeline (Supplementary Fig. 13). There was a general positive association between FC and FD regardless of the distance between ROIs; the trendline was above zero on the y-axis, but the correlation was not dependent on the distance between ROIs. That is, although the trendline was above zero, the line was perpendicular to the zero of the y-axis with no visible slope. This is likely due to the use of a low-motion sample in the current study. Low-motion samples are one of the most effective ways to combat distance-dependence effects of head motion (Parkes et al., 2018).

To further ensure that head motion was not driving GS topography changes across age, we used a multivariate partial least squares (PLS) analysis implemented in Matlab (McIntosh, Chau, & Protzner, 2004) to identify the spatial relationship between head motion and GS coupling strength across the GS topography spatial maps from the tICA preprocessing pipeline. PLS maximizes the covariance among voxels with a behavioral variable of interest that is represented by a latent variable (LV) (Supplementary Fig. 14). This LV represents the multivariate whole-brain voxel-wise spatial relationship between head motion (as measured by FD) and GS topography

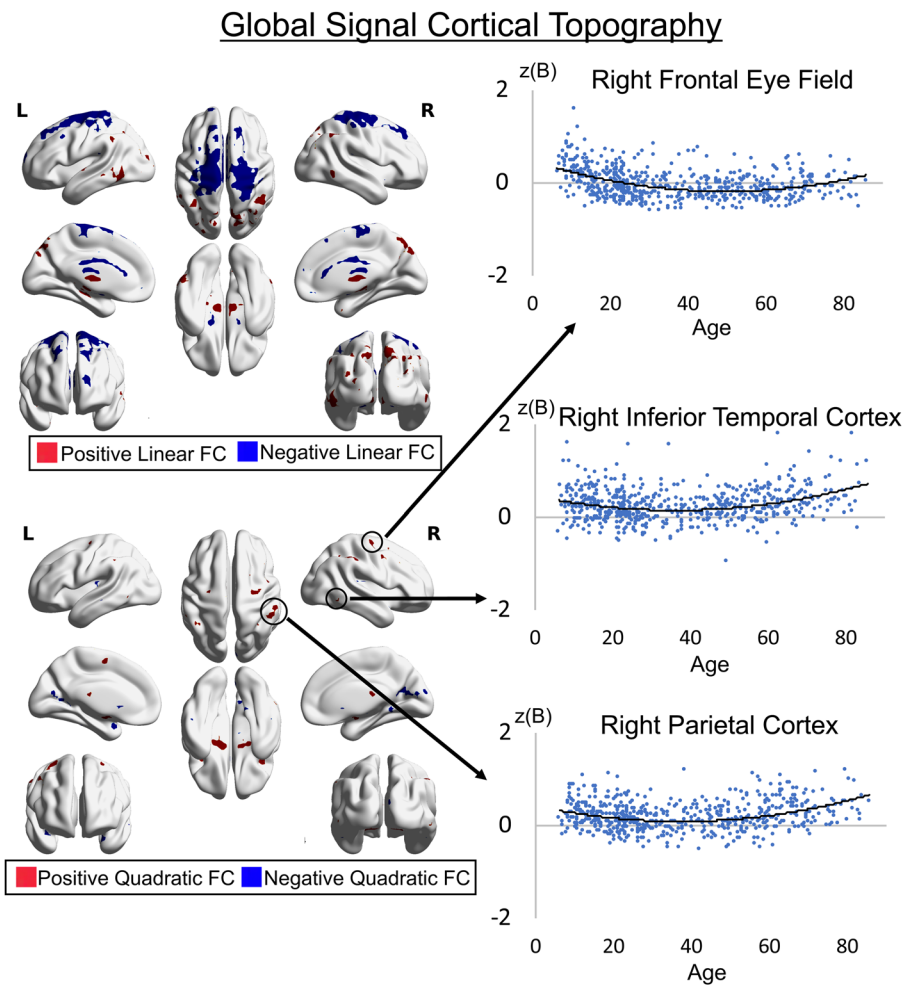

Fig. 3. Group spatial maps showing cortical associations between the global signal and voxel-wise time-series across age ($p < 0.001$ voxel-wise uncorrected and $p < 0.05$ cluster-wise corrected). Positive quadratic associations show that the GS has stronger associations with regions of the lateral frontoparietal (parietal cortex) and dorsal attention networks (frontal eye fields and inferior temporal cortex) in younger and older individuals compared with middle aged individuals. Negative linear associations show that the GS is more weakly coupled with sensorimotor areas in older individuals compared to younger individuals. Other linear associations are shown for completeness, as quadratic effects take precedence over linear effects in general linear models within the same spatial areas. The z-scored unstandardized beta is on the y-axis and age is on the x-axis.

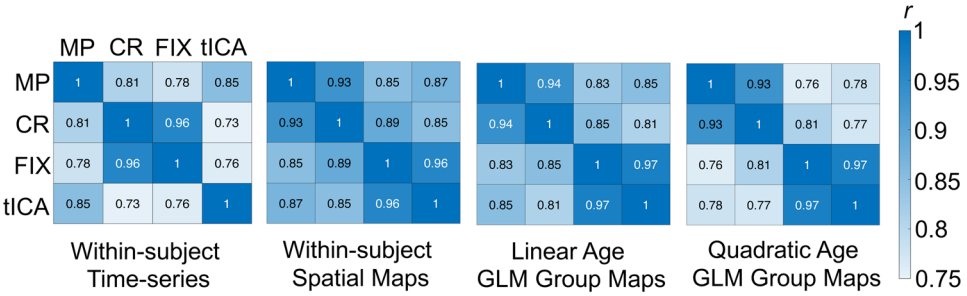

Fig. 4. Temporal and spatial correlations across preprocessing pipelines. Within-subject time-series temporal correlations and within-subject maps spatial correlations represent the influence of preprocessing pipelines across subjects without considering the influence of age. Linear age GLM and quadratic age GLM effects represent the influence of preprocessing pipelines across group GLM effects for linear age and quadratic age. All matrices show strong associations across preprocessing pipelines (rs > 0.73). MP = minimally preprocessed; CR = covariate regression; FIX = ICA-FIX, tICA = temporal ICA.

across subjects, and is differentiated from random noise using permutation testing (5000 permutations, $p < 0.05$). Each voxel within the LV is subjected to bootstrap estimation of standard errors (5000 bootstraps; approximates a p value of <0.001) to determine if the voxel score is reliably different from zero. Each subject is then assigned a "brain score" that represents how strongly that subject's data is represented within the LV. Each subject's brain score was then used as an additional nuisance regressor in the linear and quadratic GLMs assessing the association between GS topography magnitude and age, in addition to the average FD head motion and sex regressors from the original analyses. The results were unchanged from the main analyses (Supplementary Fig. 15), demonstrating that the influence of head motion on GS topography is spatially distinct from the influence of age on GS topography.

Previous research has shown that the GS is affected by the time of day when the brain scan was acquired (Orbon et al., 2020) and the state of arousal (Chang et al., 2016), so the association between subject age and the start of the MRI scan session was examined as well as possible relationships between sleep quality and age (Supplementary Fig. 1). There were 597 subjects that had a listed start time for their MRI scan session. There was no significant correlation between subject age and the start time of the MRI scan session ($p = 0.41$). This suggests that the start of the scan time should not have an influence on any of the age effects presented here.

Indexes of overall sleep quality were assessed using the Pittsburgh Sleep Quality Index (PSQI) (Buysse et al., 1989) that provides a summary measure of sleep quality based on factors such as the duration of sleep, consistency of sleep, influence of medications, and possible daytime dysfunction. There were 525 subjects that had a total PSQI score. There was no significant correlation between overall PSQI sleep quality score and age ($p = 0.19$), suggesting that differences in daytime arousal due to sleep quality across age did not influence the results.

4. DISCUSSION

Global signal regression is a widely used fMRI preprocessing step, yet this practice remains one of the most controversial topics in network neuroscience (T. T. Liu et al., 2017; Murphy & Fox, 2017; Uddin, 2020). By providing a whole-brain metric of average brain activation (i.e., the GS) coupled with individual voxel activation, GS topography represents a unique measure of intrinsic brain organization related to trait behavior, task states, and clinical diagnosis (Ao et al., 2021; Li, Kong, et al., 2019b). Our results show that associations between brain regions and the GS depend strongly on age and spatial location in the brain. We also find that GS topography associations across age are stable across multiple preprocessing pipelines, demonstrating support for GS topography as a useful way of characterizing overall brain activity and connectivity related to development. Our results demonstrate the utility of GS topography in characterizing brain organization across a significant portion of the human lifespan and also suggest that careful consideration of GS regression is warranted when age-related FC effects are of interest.

The current study showed that subcortical regions have distinct coupling patterns with the GS across early and later life stages. The thalamus presented with stronger associations with the GS across age. The thalamus has been identified as an integral initiating and mediating force of arousal and vigilance in the brain, as well as facilitating shifts in connectivity, activity, and network topology (Shine et al., 2023). Stronger thalamic coupling with the GS across age could indicate that the portion of the GS related to arousal becomes increasingly important as individuals get older. On the other hand, the thalamus has been shown to play an important role in aging and cognition in task-fMRI studies (Goldstone et al., 2018). Thus, it is possible that the thalamus plays an integrative role in both vigilance and cognitive processes across age in the context of its role in GS composition.

The nucleus basalis demonstrated stronger associations with the GS at early and late periods of life compared with middle age. Previous research has demonstrated that deactivation of the nucleus basalis via chemical intervention in macaques modulates the BOLD GS in the ipsilateral hemisphere (Turchi et al., 2018). This suggests a causal role of the nucleus basalis in cortical BOLD activity. The current study shows that the nucleus basalis has the same u-shaped pattern of coupling with the lateral frontoparietal and dorsal attention networks. Within the context of the current study, this may suggest that the contribution of nucleus basalis activity to the GS coordinates activity within the lateral frontoparietal control and dorsal attention networks. However, it is not possible to determine the causal direction of this relationship across age, as *in vivo* manipulation of the nucleus basalis is not possible to conduct safely in humans.

The current study shows quadratic patterns of associations between the GS and network nodes within the lateral frontoparietal control network and dorsal attention network. Relative to middle age, these two networks show stronger associations with the GS at early (<20 years) and later periods (>60 years) of life. The opposite pattern emerges in the medial prefrontal cortex, caudate, and lower-level visual cortices, where the association with the GS is weakest at early and later periods of life, with the strongest association with the GS in

middle age. These quadratic associations are similar to other age-FC trajectories that typically show a curvilinear pattern of network development, where within-network coupling increases while between-network coupling decreases until middle age (Fair et al., 2009). After middle age, within-network coupling increases while within-network decreases (Betzel et al., 2014; Chan et al., 2014; Vij et al., 2018). The trajectory of the lateral frontoparietal network also closely resembles executive function performance across development, where performance peaks in the 3rd and 4th decade of life before dropping off in old age (Ferguson et al., 2021). Taken together, curvilinear trajectories of network integration and segregation, as well as executive function behavioral performance show similar curvilinear trajectories as the lateral frontoparietal control network. Thus, our results support a dual-layer model of GS composition that demonstrates linear cross-sectional changes within the thalamus and sensorimotor regions as part of the background arousal layer against quadratic cross-sectional lateral frontoparietal control network changes in the foreground cortico-cortical cognition layer.

These results are in accord with the dual-layer model of GS composition (Zhang & Northoff, 2022) that proposes a subcortical-cortical background layer associated with arousal and vigilance via the thalamus and basal forebrain (X. Liu et al., 2018) and a cortico-cortical foreground layer associated with network organization and cognitive rest-task states (Zhang et al., 2020). Within the context of the current study, we find that subcortical and cortical contributions to the GS vary according to age. In early life, the GS shows stronger associations with the putamen, caudate nucleus, lateral frontoparietal control network, and the dorsal attention network. In middle age, the associations between these regions and the GS is weakest, with only the thalamus showing increased association with the GS. Finally, in old age, all subcortical and cortical regions show strong association with the GS, with the exception of the putamen which shows its weakest association with the GS in older age. These differing patterns across age suggest that the contribution of various brain regions to the GS changes across human development. The changing composition of brain activity contributing to the GS across early and later life may be an attempt at optimizing arousal and vigilance processes of the background subcortical-cortical layer with cognitive processes of the cortical foreground layer. Future studies will need to examine the mechanisms driving these associations by identifying how differing levels of brain activity may be driving relationships with the GS time-series and in turn, influencing GS topography.

Our results also complement a recent study describing changes in the GS across age from 19 to 80 years of age (Ao et al., 2022). Increasing age was shown to be associated with a reduction in GS variability, in accord with previous research showing that variability generally decreases across most of the brain with age (Garrett et al., 2010; Nomi et al., 2017). The GS also showed a shift from lower frequencies to higher frequencies across age, in accord with functional network connectivity studies of aging (Vij et al, 2018). Finally, the GS in older individuals presented with a more evenly distributed power-frequency relationship compared with the GS in younger individuals. As the GS is a sum of all brain activity, changes in the GS across age also reflect changes in overall brain function. Taken together, changes in the GS and its associated topography show distinct age-related changes that should be taken into consideration when interpreting studies using GS regression.

The systematic trajectories of GS topography across age make interpretation of studies using GS regression and age as a variable of interest complicated. As the age range of the sample increases, there is a greater possibility that different brain regions and networks will be influenced by GS regression. For example, GS regression may have a greater influence on the lateral frontoparietal network in younger and older age samples compared with middle age samples. Additionally, GS regression on young individuals may not influence thalamic and occipital cortex activity as much as GS regression on older adults. Thus, GS regression may have system-specific implications in categorical and dimensional fMRI age investigations. Further compounding these issues is that it is unknown if GS regression will be beneficial or detrimental for identifying cognition related brain activity. That is, it is not possible to determine if the GS is driving activity in specific networks, or if specific network activity is driving the global signal in an age-dependent manner. GS regression would be beneficial in the former case, but detrimental in the latter. Currently, the underlying physiological and neuronal contributions to the global signal remain unknown.

Future studies should carefully consider the implementation of GS regression, as its application may have important influences on analysis results. There may be additional factors to consider when deciding if to apply GS regression to studies exploring aging effects. This may include the types of artifact in the data and how well GS regression removes the artifacts in question. For example, while GS regression may be effective in removing certain respiratory and cardiac artifacts within the BOLD signal, head motion may be better addressed using low-motion samples or scrubbing. Respiratory and cardiac effects may also be better addressed using spatial and temporal ICA denoising. Finally, multi-echo ICA denoising has shown to be effective at removing artifacts related to the GS while leaving neural signals untouched (Setton et al., 2022;

Spreng et al., 2019). Each dataset contains its own unique artifactual properties, and the choice of preprocessing pipeline should consider how to best address various types of noise within the BOLD signal.

4.1. Limitations and future directions

Although previous research suggests that temporal ICA denoising effectively removes structured global artifacts such as head motion, respiration, and cardiac events from resting-state fMRI data (Glasser et al., 2018), it is still possible that unstructured spatial and temporal noise has an influence on age associations with GS topography and its lifespan associations. Importantly however, the significant change of GS composition between FIX and tICA preprocessing pipelines, combined with the fact that the GS topography effects remained virtually unchanged, suggests that GS topography is somewhat robust to such artifacts. Additionally, it is unclear if one would want to completely remove aspects of respiration and cardiac activity associated with neural function as they play an important role in the dual-layer model of GS composition (Zhang & Northoff, 2022) as they are intricately linked with the GS (Bolt et al., 2023). These factors along with previous research showing that the GS is strongly associated with brain network activity (Gotts et al., 2020) and behavioral traits (Li, Kong, et al., 2019) show how GS topography can be of further interest to neuroscientists as a biologically important aspect of brain function.

Future studies are needed to replicate the findings in additional datasets, extend the results even further to individuals outside of the 6-85 year age range of the current study, and further disentangle possible higher order non-linear associations. Datasets that cover the entirety of the lifespan from fetal stage to late life stages are needed to further elucidate the development of the GS and its associated topography. Infant and fetal scanning are becoming increasingly common, which will eventually allow for a more complete description of the evolution of GS topography. Additionally, higher-order modeling of non-linear associations and shorter age-ranges for cross-sectional groups would allow for a more complete characterization of GS topography changes. The current study represents one of the first steps in charting the development of the GS and its associated spatially distributed topography.

The current results also open up further avenues of possible exploration with regards to the impact of GS regression on aging studies using different types of analytical methodologies. For example, aging effects of brain function have been shown using a number of approaches such as functional connectivity gradients (Bethlehem et al., 2020), graph theory (Wright et al., 2021), brain signal variability (Nomi et al., 2017), and ICA algorithms (Vij et al., 2018). Future studies should examine the relationships between the impact of GS regression on the aging brain's functional architecture. Identifying the effects of regression of a global aspect of brain function will provide greater insight into how preprocessing choice, analysis choice, and brain function interact across age.

5. CONCLUSIONS

In conclusion, we show that age is significantly associated with the spatial topography of the GS in resting-state fMRI data. The thalamus and sensorimotor regions show distinct linear cross-sectional aging patterns compared with the quadratic aging patterns found for the lateral frontoparietal control network. Our results support a dual-layer view of the GS where composition of the GS may include a subcortical-cortical background layer modulating arousal via the thalamus and a cortico-cortical foreground layer modulating cognition via the lateral frontoparietal network that diverge as linear and quadratic effects across early and later life stages. Due to the importance and unabated controversy over GS regression, researchers should be cautious when considering the implications of its application. As the field of fMRI keeps maturing, understanding how GS regression may help or hinder statistical analyses, and potentially mask true age-related FC effects, will continue to be of paramount importance.

DATA AND CODE AVAILABILITY

All data are available for download from the Enhanced Nathan Kline Institute - Rockland Sample data repository (http://fcon_1000.projects.nitrc.org/indi/enhanced/).

Code used in analyses available on Github: https://github.com/jasonSnomi/LifespanGlobalSignalTopography

AUTHOR CONTRIBUTIONS

J.S.N. conceived of the project, helped with data preprocessing, conducted all analyses, and wrote the manuscript. D.B. and L.Q.U. conceived of the project, consulted on analyses, and helped write the manuscript. J.L., B.T.T.Y, and C.C. consulted on the analyses and helped write the manuscript. S.K. and Z.T.G. helped to download, sort, and preprocess the resting-state data. T.B. and R.N.S. contributed to the data analysis and helped to write the manuscript.

DECLARATION OF COMPETING INTEREST

The authors have no conflicts to report.

ACKNOWLEDGEMENTS

J.S.N. is supported by R21HD111805 from NICHD. B.T.T.Y. is supported by the NUS Yong Loo Lin School of Medicine (NUHSRO/2020/124/TMR/LOA), the Singapore National Medical Research Council (NMRC) LCG (OFLC-G19May-0035), NMRC CTG-IIT (CTGIIT23jan-0001), NMRC STaR (STaR20nov-0003), Singapore Ministry of Health (MOH) Centre Grant (CG21APR1009), the Temasek Foundation (TF2223-IMH-01), and NIMH (R01MH120080 & R01MH133334). L.Q.U. is supported by R21HD111805 from NICHD and U01DA050987 from NIDA. Any opinions, findings, and conclusions or recommendations expressed in this material are those of the authors and do not reflect the views of the Singapore NRF, NMRC, MOH or Temasek Foundation.

SUPPLEMENTARY MATERIALS

Supplementary material for this article is available with the online version here: https://doi.org/10.1162/imag_a_00101.

REFERENCES

Ao, Y., Kou, J., Yang, C., Wang, Y., Huang, L., Jing, X., Cui, Q., Cai, X., & Chen, J. (2022). The temporal dedifferentiation of global brain signal fluctuations during human brain ageing. *Scientific Reports*, *12*(1), 3616. https://doi.org/10.1038/s41598-022-07578-6

Ao, Y., Ouyang, Y., Yang, C., & Wang, Y. (2021). Global signal topography of the human brain: A novel framework of functional connectivity for psychological and pathological investigations. *Frontiers in Human Neuroscience*, *15*, 644892. https://www.frontiersin.org/articles/10.3389/fnhum.2021.644892

Bethlehem, R. A. I., Paquola, C., Seidlitz, J., Ronan, L., Bernhardt, B., Consortium, C.-C., & Tsvetanov, K. A. (2020). Dispersion of functional gradients across the adult lifespan. *NeuroImage*, *222*, 117299. https://doi.org/10.1016/j.neuroimage.2020.117299

Betzel, R. F., Byrge, L., He, Y., Goñi, J., Zuo, X.-N., & Sporns, O. (2014). Changes in structural and functional connectivity among resting-state networks across the human lifespan. *NeuroImage*, *102*, 345–357. https://doi.org/10.1016/j.neuroimage.2014.07.067

Bolt, T., Nomi, J. S., Bzdok, D., Salas, J. A., Chang, C., Thomas Yeo, B. T., Uddin, L. Q., & Keilholz, S. D. (2022). A parsimonious description of global functional brain organization in three spatiotemporal patterns. *Nature Neuroscience*, *25*(8), 1093–1103. https://doi.org/10.1038/s41593-022-01118-1

Bolt, T., Wang, S., Nomi, J. S., Setton, R., Gold, B. P., deB. Frederick, B., Spreng, R. N., Keilholz, S. D., Uddin, L. Q., & Chang, C. (2023). A unified physiological process links global patterns of functional MRI, respiratory activity, and autonomic signaling. *bioRxiv* 2023–01.

Buysse, D. J., Reynolds, C. F., Monk, T. H., Berman, S. R., & Kupfer, D. J. (1989). The Pittsburgh sleep quality index: A new instrument for psychiatric practice and research. *Psychiatry Research*, *28*(2), 193–213. https://doi.org/10.1016/0165-1781(89)90047-4

Chan, M. Y., Park, D. C., Savalia, N. K., Petersen, S. E., & Wig, G. S. (2014). Decreased segregation of brain systems across the healthy adult lifespan. *Proceedings of the National Academy of Sciences*, *111*(46), E4997–E5006. https://doi.org/10.1073/pnas.1415122111

Chang, C., Leopold, D. A., Schölvinck, M. L., Mandelkow, H., Picchioni, D., Liu, X., Ye, F. Q., Turchi, J. N., & Duyn, J. H. (2016). Tracking brain arousal fluctuations with fMRI. *Proceedings of the National Academy of Sciences*, *113*(16), 4518–4523. https://doi.org/10.1073/pnas.1520613113

Ciric, R., Rosen, A. F. G., Erus, G., Cieslak, M., Adebimpe, A., Cook, P. A., Bassett, D. S., Davatzikos, C., Wolf, D. H., & Satterthwaite, T. D. (2018). Mitigating head motion artifact in functional connectivity MRI. *Nature Protocols*, *13*(12), 2801–2826. https://doi.org/10.1038/s41596-018-0065-y

Ciric, R., Wolf, D. H., Power, J. D., Roalf, D. R., Baum, G. L., Ruparel, K., Shinohara, R. T., Elliott, M. A., Eickhoff, S. B., Davatzikos, C., Gur, R. C., Gur, R. E., Bassett, D. S., & Satterthwaite, T. D. (2017). Benchmarking of participant-level confound regression strategies for the control of motion artifact in studies of functional connectivity. *NeuroImage*, *154*, 174–187. https://doi.org/10.1016/j.neuroimage.2017.03.020

Fair, D. A., Cohen, A. L., Power, J. D., Dosenbach, N. U. F., Church, J. A., Miezin, F. M., Schlaggar, B. L., & Petersen, S. E. (2009). Functional brain networks develop from a "local to distributed" organization. *PLOS Computational Biology*, *5*(5), e1000381. https://doi.org/10.1371/journal.pcbi.1000381

Ferguson, H. J., Brunsdon, V. E. A., & Bradford, E. E. F. (2021). The developmental trajectories of executive function from adolescence to old age. *Scientific Reports*, *11*(1), 1382. https://doi.org/10.1038/s41598-020-80866-1

Friston, K. J., Williams, S., Howard, R., Frackowiak, R. S. J., & Turner, R. (1996). Movement-related effects in fMRI time-series: Movement artifacts in fMRI. *Magnetic Resonance in Medicine*, *35*(3), 346–355. https://doi.org/10.1002/mrm.1910350312

Garrett, D. D., Kovacevic, N., McIntosh, A. R., & Grady, C. L. (2010). Blood oxygen level-dependent signal variability is more than just noise. *Journal of Neuroscience*, *30*(14), 4914–4921. https://doi.org/10.1523/JNEUROSCI.5166-09.2010

Glasser, M. F., Coalson, T. S., Bijsterbosch, J. D., Harrison, S. J., Harms, M. P., Anticevic, A., Van Essen, D. C., & Smith, S. M. (2018). Using temporal ICA to selectively remove global noise while preserving global signal in functional MRI data. *NeuroImage*, *181*, 692–717. https://doi.org/10.1016/j.neuroimage.2018.04.076

Goldstone, A., Mayhew, S. D., Hale, J. R., Wilson, R. S., & Bagshaw, A. P. (2018). Thalamic functional connectivity and its association with behavioral performance in older age. *Brain and Behavior*, *8*(4), e00943. https://doi.org/10.1002/brb3.943

Gotts, S. J., Gilmore, A. W., & Martin, A. (2020). Brain networks, dimensionality, and global signal averaging in resting-state fMRI: Hierarchical network structure results in low-dimensional spatiotemporal dynamics. *NeuroImage*, *205*, 116289. https://doi.org/10.1016/j.neuroimage.2019.116289

Griffanti, L., Douaud, G., Bijsterbosch, J., Evangelisti, S., Alfaro-Almagro, F., Glasser, M. F., Duff, E. P., Fitzgibbon, S., Westphal, R., Carone, D., Beckmann, C. F., & Smith, S. M. (2017). Hand classification of fMRI ICA noise components. *NeuroImage*, *154*, 188–205. https://doi.org/10.1016/j.neuroimage.2016.12.036

Griffanti, L., Salimi-Khorshidi, G., Beckmann, C. F., Auerbach, E. J., Douaud, G., Sexton, C. E., Zsoldos, E., Ebmeier, K. P., Filippini, N., Mackay, C. E., Moeller, S., Xu, J., Yacoub, E., Baselli, G., Ugurbil, K., Miller, K. L., & Smith, S. M. (2014). ICA-based artefact removal and accelerated fMRI acquisition for improved resting state network imaging. *NeuroImage*, *95*, 232–247. https://doi.org/10.1016/j.neuroimage.2014.03.034

Li, J., Bolt, T., Bzdok, D., Nomi, J. S., Yeo, B. T. T., Spreng, R. N., & Uddin, L. Q. (2019). Topography and behavioral relevance of the global signal in the human brain. *Scientific Reports*, *9*(1), 14286. https://doi.org/10.1038/s41598-019-50750-8

Li, J., Kong, R., Liégeois, R., Orban, C., Tan, Y., Sun, N., Holmes, A. J., Sabuncu, M. R., Ge, T., & Yeo, B. T. T. (2019). Global signal regression strengthens association between resting-state functional connectivity and behavior. *NeuroImage*, *196*, 126–141. https://doi.org/10.1016/j.neuroimage.2019.04.016

Liu, T. T., Nalci, A., & Falahpour, M. (2017). The global signal in fMRI: Nuisance or Information? *NeuroImage*, *150*, 213–229. https://doi.org/10.1016/j.neuroimage.2017.02.036

Liu, X., de Zwart, J. A., Schölvinck, M. L., Chang, C., Ye, F. Q., Leopold, D. A., & Duyn, J. H. (2018). Subcortical evidence for a contribution of arousal to fMRI studies of brain activity. *Nature Communications*, *9*(1), 395. https://doi.org/10.1038/s41467-017-02815-3

Ma, Y., Ma, Z., Liang, Z., Neuberger, T., & Zhang, N. (2020). Global brain signal in awake rats. *Brain Structure and Function*, *225*(1), 227–240. https://doi.org/10.1007/s00429-019-01996-5

McIntosh, A. R., Chau, W. K., & Protzner, A. B. (2004). Spatiotemporal analysis of event-related fMRI data using partial least squares. *NeuroImage*, *23*(2), 764–775. https://doi.org/10.1016/j.neuroimage.2004.05.018

Murphy, K., & Fox, M. D. (2017). Towards a consensus regarding global signal regression for resting state functional connectivity MRI. *NeuroImage*, *154*, 169–173. https://doi.org/10.1016/j.neuroimage.2016.11.052

Nomi, J. S., Bolt, T. S., Ezie, C. E. C., Uddin, L. Q., & Heller, A. S. (2017). Moment-to-moment bold signal variability reflects regional changes in neural flexibility across the lifespan. *Journal of Neuroscience*, *37*(22), 5539–5548. https://doi.org/10.1523/JNEUROSCI.3408-16.2017

Nooner, K., Colcombe, S., Tobe, R., Mennes, M., Benedict, M., Moreno, A., Panek, L., Brown, S., Zavitz, S., Li, Q., Sikka, S., Gutman, D., Bangaru, S., Schlachter, R. T., Kamiel, S., Anwar, A., Hinz, C., Kaplan, M., Rachlin, A., … Milham, M. (2012). The NKI-rockland sample: A model for accelerating the pace of discovery science in psychiatry. *Frontiers in Neuroscience*, *6*. https://www.frontiersin.org/articles/10.3389/fnins.2012.00152

Orban, C., Kong, R., Li, J., Chee, M. W. L., & Yeo, B. T. T. (2020). Time of day is associated with paradoxical reductions in global signal fluctuation and functional connectivity. *PLoS Biology*, *18*(2), e3000602. https://doi.org/10.1371/journal.pbio.3000602

Parkes, L., Fulcher, B., Yücel, M., & Fornito, A. (2018). An evaluation of the efficacy, reliability, and sensitivity of motion correction strategies for resting-state functional MRI. *NeuroImage*, *171*, 415–436. https://doi.org/10.1016/j.neuroimage.2017.12.073

Power, J. D., Barnes, K. A., Snyder, A. Z., Schlaggar, B. L., & Petersen, S. E. (2012). Spurious but systematic correlations in functional connectivity MRI networks arise from subject motion. *NeuroImage*, *59*(3), 2142–2154. https://doi.org/10.1016/j.neuroimage.2011.10.018

Power, J. D., Plitt, M., Laumann, T. O., & Martin, A. (2017). Sources and implications of whole-brain fMRI signals in humans. *NeuroImage*, *146*, 609–625. https://doi.org/10.1016/j.neuroimage.2016.09.038

Salimi-Khorshidi, G., Douaud, G., Beckmann, C. F., Glasser, M. F., Griffanti, L., & Smith, S. M. (2014). Automatic denoising of functional MRI data: Combining independent component analysis and hierarchical fusion of classifiers. *NeuroImage*, *90*, 449–468. https://doi.org/10.1016/j.neuroimage.2013.11.046

Schaefer, A., Kong, R., Gordon, E. M., Laumann, T. O., Zuo, X.-N., Holmes, A. J., Eickhoff, S. B., & Yeo, B. T. T. (2018). Local-global parcellation of the human cerebral cortex from intrinsic functional connectivity MRI. *Cerebral Cortex (New York, NY)*, *28*(9), 3095–3114. https://doi.org/10.1093/cercor/bhx179

Schölvinck, M. L., Maier, A., Ye, F. Q., Duyn, J. H., & Leopold, D. A. (2010). Neural basis of global resting-state fMRI activity. *Proceedings of the National Academy of Sciences*, *107*(22), 10238–10243. https://doi.org/10.1073/pnas.0913110107

Setton, R., Mwilambwe-Tshilobo, L., Girn, M., Lockrow, A. W., Baracchini, G., Hughes, C., Lowe, A. J., Cassidy, B. N., Li, J., Luh, W.-M., Bzdok, D., Leahy, R. M., Ge, T., Margulies, D. S., Misic, B., Bernhardt, B. C., Stevens, W. D., De Brigard, F., Kundu, P., … Spreng, R. N. (2022). Age differences in the functional architecture of the human brain. *Cerebral Cortex (New York, NY)*, *33*(1), 114–134. https://doi.org/10.1093/cercor/bhac056

Shine, J. M., Lewis, L. D., Garrett, D. D., & Hwang, K. (2023). The impact of the human thalamus on brain-wide information processing. *Nature Reviews Neuroscience*, *24*(7), 416–430. https://doi.org/10.1038/s41583-023-00701-0

Smith, S. M., Miller, K. L., Moeller, S., Xu, J., Auerbach, E. J., Woolrich, M. W., Beckmann, C. F., Jenkinson, M., Andersson, J., Glasser, M. F., Van Essen, D. C., Feinberg, D. A., Yacoub, E. S., & Ugurbil, K. (2012). Temporally-independent functional modes of spontaneous brain activity. *Proceedings of the National Academy of Sciences*, *109*(8), 3131–3136. https://doi.org/10.1073/pnas.1121329109

Spreng, R. N., Fernández-Cabello, S., Turner, G. R., & Stevens, W. D. (2019). Take a deep breath: Multiecho fMRI denoising effectively removes head motion artifacts, obviating the need for global signal regression. *Proceedings of the National Academy of Sciences*, *116*(39), 19241–19242. https://doi.org/10.1073/pnas.1909848116

Turchi, J., Chang, C., Ye, F. Q., Russ, B. E., Yu, D. K., Cortes, C. R., Monosov, I. E., Duyn, J. H., & Leopold, D. A. (2018). The basal forebrain regulates global resting-state fmri fluctuations. *Neuron*, *97*(4), 940–952.e4. https://doi.org/10.1016/j.neuron.2018.01.032

Uddin, L. Q. (2020). Bring the noise: Reconceptualizing spontaneous neural activity. *Trends in Cognitive Sciences*, *24*(9), 734–746. https://doi.org/10.1016/j.tics.2020.06.003

Vij, S. G., Nomi, J. S., Dajani, D. R., & Uddin, L. Q. (2018). Evolution of spatial and temporal features of functional brain networks across the lifespan. *NeuroImage*, *173*, 498–508. https://doi.org/10.1016/j.neuroimage.2018.02.066

Wright, L. M., De Marco, M., & Venneri, A. (2021). A graph theory approach to clarifying aging and disease related changes in cognitive networks. *Frontiers in Aging Neuroscience*, *13*. https://www.frontiersin.org/articles/10.3389/fnagi.2021.676618

Yan, C., & Zang, Y. (2010). DPARSF: A MATLAB toolbox for "pipeline" data analysis of resting-state fMRI. *Frontiers in Systems Neuroscience*, *4*. https://www.frontiersin.org/articles/10.3389/fnsys.2010.00013

Zhang, J., Huang, Z., Tumati, S., & Northoff, G. (2020). Rest-task modulation of fMRI-derived global signal topography is mediated by transient coactivation patterns. *PLoS Biology*, *18*(7), e3000733. https://doi.org/10.1371/journal.pbio.3000733

Zhang, J., & Northoff, G. (2022). Beyond noise to function: Reframing the global brain activity and its dynamic topography. *Communications Biology*, *5*(1), 1–12. https://doi.org/10.1038/s42003-022-04297-6